Control of Energy Dissipation and Photochemical Activity in Photosystem I by NADP-Dependent Reversible Conformational Changes†

Subramanyam Rajagopal,‡ Nikolai G. Bukhov,‡,§ Heidar-Ali Tajmir-Riahi,‡ and Robert Carpentier*,‡

Groupe de Recherche en Énergie et Information Biomoléculaires, Université du Québec à Trois-Rivières, C.P. 500 Trois-Rivières, Québec, Canada G9A 5H7, and K. A. Timiriazev Institute of Plant Physiology, Russian Academy of Science, Botanicheskaya 35, 127276 Moscow, Russia

Received June 3, 2003; Revised Manuscript Received August 13, 2003

ABSTRACT: Addition of $NADP^+$ to thylakoid membranes or isolated photosystem I (PSI) submembrane fractions quenched chlorophyll fluorescence by up to 40% at low or room temperature. This quenching was reversed by NADPH. Similar quenching was also observed with the addition of heparin or thenoyltrifluoroacetone (TTFA), inhibitors that bind ferredoxin:$NADP^+$ reductase (FNR) and prevent reduction of $NADP^+$. The $NADP^+$-induced quenching coincided with a reversible conformational change of the secondary protein structure in the PSI submembrane fractions where 20% of the α-helix conformations were transformed mainly into β-sheet-like structures. Further, P700 photooxidation was retarded due to this conformational change, and about 25% of the centers could not be photooxidized, these changes being also reversible with addition of NADPH. The above modifications in the presence of $NADP^+$ also increased photodamage processes under strong illumination, and NADPH protected it. Conformational modification of FNR upon binding of $NADP^+$ or NADPH is proposed to trigger the macromolecular changes in a larger part of the protein complex of PSI. The conformational changes must increase the intermolecular distances and change the mutual orientation between the various cofactors in the PSI complex. This new control mechanism of energy dissipation and photochemical activity by $NADP^+$/NADPH is proposed to increase the turnover rate of PSI under conditions when both linear and cyclic electron transport activities must be supported.

In chloroplasts of higher plants and algae, photosystem I (PSI)[1] catalyzes the light-driven electron transport between plastocyanin and ferredoxin. The enzyme ferredoxin:$NADP^+$ reductase (FNR) is required for the reduction of $NADP^+$ to NADPH in a reaction that uses two molecules of reduced ferredoxin. PSI is formed of a core complex composed of an heterodimer of the PsaA/PsaB polypeptides surrounded by the peripheral chlorophyll (Chl) *a*/*b* binding proteins (LHCI) and at least 12 other polypeptide subunits (*1*, *2*). The reaction center of PSI, P700, is located in the PsaA/PsaB protein complex with the primary electron acceptors and about 90−100 Chl and 15−22 β-carotene molecules as determined for higher plants and cyanobacteria (*1*, *3*). LHCI is composed of two subcomplexes, LHCI-680 that consists of two polypeptides of 23 kDa (Lhca2) and 25 kDa (Lhca3), respectively, and LHCI-730 that also comprises two polypeptides of 22 kDa (Lhca1) and 21 kDa (Lhca4), respectively (*4*, *5*).

The rate of electron transport within PSI is mainly controlled by the flux of electrons transferred from photosystem II (PSII) through the cytochrome b_6/f complex and by the activity of dark carbon metabolism that uses NADPH formed at the acceptor side of PSI (*6*−*9*). It is also known that the ATP/NADPH ratio can be modulated by the onset of cyclic electron transport around PSI, which produces ATP without the reduction of $NADP^+$ molecules (*10*). Thus an increased chloroplastic concentration of NADPH is proposed to poise the redox state of the intersystem electron carriers and favor cyclic PSI electron transport (*11*). Migration of the phospho-LHCII complex from PSII during state 2 to state 1 transition controls excitation energy in PSII and was reported to slightly increase the antenna cross-section in PSI (*12*, *13*). However, there is no report indicating nonphotochemical control of energy dissipation and photochemistry in PSI such as the energy-dependent nonphotochemical quenching observed in PSII. The latter is initiated by the formation of a pH gradient across the thylakoid membrane and the transformation of violaxanthin to zeaxathin during the so-called xanthophyll cycle (*12*, *14*). These mechanisms are often associated with photoprotection together with other structural adaptation processes (*15*). Even though PSII was reported to be more sensitive than PSI to strong illumination (*16*, *17*), several studies indicated that PSI is equally sensitive to light (*18*). Thus, besides the basic availability of reduced donors and oxidized electron acceptors for P700, other mechanisms are expected that would have a better control over energy dissipation and photochemical activity in PSI.

† This research was supported by the Natural Sciences and Engineering Research Council of Canada and by Fonds Québécois de la Recherche sur la Nature et les Technologies.

* To whom correspondence and reprint requests should be addressed. E-mail: Robert_Carpentier@uqtr.ca. Phone: 1-819-376-5011. Fax: 1-819-376-5057.

‡ Université du Québec à Trois-Rivières.

§ K. A. Timiriazev Institute of Plant Physiology.

[1] Abbreviations: Chl, chlorophyll; FNR, ferredoxin:$NADP^+$ reductase; LHC, light harvesting complex; P700, primary electron donor; PSI, photosystem I; PSII, photosystem II; TTFA, thenoyltrifluoroacetone.

10.1021/bi034949k CCC: $25.00
Published on Web 09/16/2003

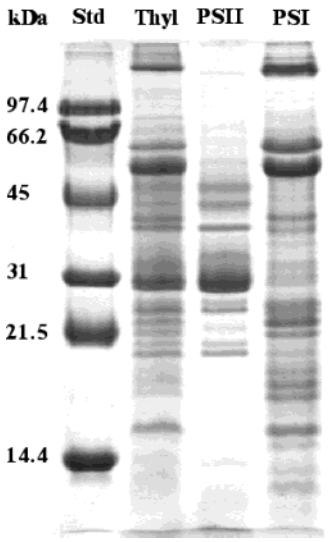

FIGURE 1: Comparison of the polypeptide profile using polyacrylamide gel electrophoresis of whole thylakoid membranes and photosystem I and II submembrane fractions isolated as described in Materials and Methods.

In this report, we present the first demonstration of a nonphotochemical type of fluorescence quenching in PSI that is promoted by $NADP^+$. A significant fluorescence quenching was observed in either whole thylakoid membranes or isolated PSI submembrane fractions in the presence of $NADP^+$ that was fully reversible with NADPH. This control of energy dissipation coincided with reversible protein conformational changes and modulation of the rate of P700 photooxidation. It is suggested that this mechanism could increase the turnover rate of PSI under conditions when both linear and cyclic electron transport activities must be supported by the photosystem.

MATERIALS AND METHODS

Isolation of Thylakoid Membranes. Thylakoid membranes were isolated from market spinach leaves and 10-day-old pea leaves grown on vermiculite as described by Goetze and Carpentier (*19*). The final pellet was resuspended in 20 mM Hepes−NaOH, 330 mM sorbitol, 10 mM NaCl, and 5 mM $MgCl_2$.

Isolation of Photosystem II Submembrane Fractions. PSII submembrane fractions were isolated from spinach leaves obtained from a local market according to Berthold et al. (*20*) with the modification described elsewhere (*21*). PSII preparations were finally suspended (2 mg of Chl/mL) in 20 mM MES−NaOH (pH 6.2), 400 mM sucrose, 15 mM NaCl, and 5 mM $MgCl_2$ and stored at −80 °C until use. The preparations were devoid of PSI polypeptides as shown in Figure 1.

Isolation of Photosystem I Submembrane Fractions. PSI submembrane fractions were isolated from fresh spinach according to the procedure of Peters et al. (*22*) with some modifications (*23*). The isolated fractions with approximately 1−2 mg of Chl/mL were suspended in a medium containing 20 mM Tricine−KOH buffer (pH 7.8), 10 mM NaCl, 10 mM KCl, and 5 mM $MgCl_2$ and stored at −80 °C until use. The Chl *a*/*b* ratios in the preparations were higher than 6.0. Chl content was determined with 80% acetone according to Porra et al. (*24*). These preparations were devoid in PSII polypeptides as shown in Figure 1.

Analysis of Polypeptide Composition. The polypeptides of thylakoid membranes and submembrane fractions were separated by sodium dodecyl sulfate−urea−polyacrylamide gel electrophoresis according to the procedure of Hui et al. (*25*). Electrophoresis was performed on 13% separating and 4% stacking gels of polyacrylamide. Aliquots of photosynthetic membranes containing 5 μg of Chl were added to equal volumes of 2× buffer (0.25 mM Tris-HCl, pH 6.8, 2% sodium dodecyl sulfate) and incubated for 30 min at 4 °C. The gels were stained with Coomassie brilliant blue R-250 and observed with a Bio-Rad Gel-Doc 2000 system.

Fluorescence Spectroscopy. Room temperature (298 K) and low-temperature (77 K) spectra of fluorescence emission excited at 436 nm were measured as reported previously (*26*) using a Perkin-Elmer LS55 spectrofluorometer. The Chl content of the samples was adjusted to 5 μg/mL. Low-temperature spectra were measured in the presence of 60% glycerol. Reversible changes of fluorescence at fixed emission wavelength (684 nm) were measured at room temperature with the addition of 100 μM $NADP^+$ (N-0505; Sigma, St. Louis, MO) and subsequent addition of 100 μM NADPH (N-1630; Sigma, St. Louis, MO).

FTIR Spectroscopy and Data Treatment. The suspensions of PSI submembrane fractions were transferred onto an AgBr window after the addition of a given concentration of appropriate additive as mentioned in the text and air-dried at room temperature under green light to form an uniform (hydrated) film. The infrared spectra were recorded using a Fourier transform infrared (FTIR) spectrometer equipped with a HgCdTe detector and a KBr beam splitter (Nicolet, Madison, WI). The spectra were taken with a resolution of 2 cm^{-1}. The secondary structure of PSI proteins was determined from the shape of the amide I band (*27*, *28*). Fourier self-deconvolution and second derivative resolution enhancement and curve-fitting procedures were applied to determine quantitatively the protein conformation. The detailed spectral treatments and calculations of protein secondary structure have been reported previously (*28*). The spectral manipulations were performed with the Gram 32 program (Galactic Industries Co., Salem, NH). Some experiments were done in D_2O to clearly determine the random component.

P700 Photooxidation Measurements. The changes in the redox state of P700, primary donor of PSI, were monitored with the absorbance changes at 830 nm (ΔA_{830}) using the dual-wavelength unit ED-P700DW of a PAM fluorometer (Walz, Effeltrich, Germany) as described in ref *29*. White actinic light was obtained from the KL 1500 projector (Walz, Effeltrich, Germany). Ascorbate (200 μM) was added to the PSI submembrane fractions (15 μg of Chl) prior to ΔA_{830} measurements to ensure complete reduction of P700 in the dark.

Strong Light Treatments. Suspensions of isolated PSI submembrane fractions containing 500 μg of Chl/mL were kept at 4 °C under continuous stirring. The fractions were irradiated for various periods of time with an intense white light (2000 μE m^{-2} s^{-1}) provided by a 150 W quartz−halogen projector lamp. White light was passed through a 5 cm layer of water containing 4% $CuSO_4$ to eliminate heat radiation. The aliquots of 30 μL were taken from the suspension every 0.5 h during the photoinhibitory treatment to assess Chl concentration and the magnitude of light-induced absorbance changes at 830 nm (ΔA_{830}).

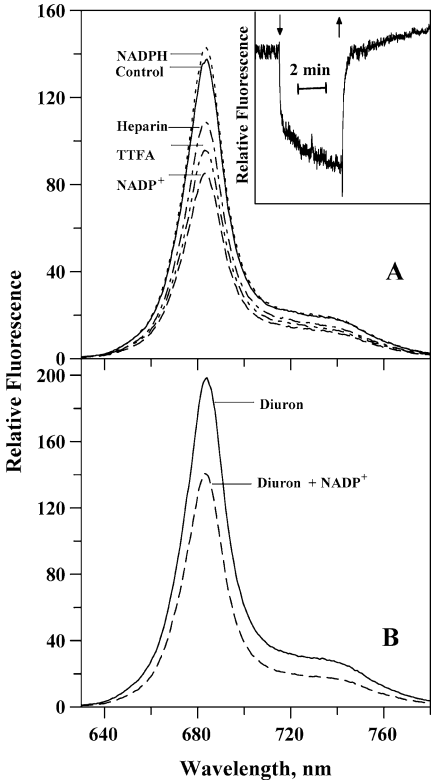

FIGURE 2: (A) Changes in the room temperature emission spectra of thylakoids with the addition of 100 μM $NADP^+$, 100 μM NADPH, 100 μM TTFA, or 20 μM heparin. Insert: Reversible fluorescence changes at 684 nm. Downward and upward arrows indicate the addition of 100 μM $NADP^+$ and 100 μM NADPH, respectively, during measurement. (B) Effect of 100 μM $NADP^+$ on the emission spectra of thylakoids in the presence of 10 μM diuron. The excitation and emission slit widths were set at 5 and 2.5 nm, respectively. These experiments were repeated in five different isolations and yielded identical spectra (the variation in intensity was below 5%); a typical spectrum is presented.

RESULTS

Figure 2A presents Chl fluorescence emission traces measured at room temperature (298 K) in thylakoid membranes isolated from spinach. Similar data were obtained with pea thylakoids. The control samples presented a maximal emission in the red at 684 nm with excitation at 436 nm. Both reduced and oxidized forms of NADP affected fluorescence intensity. Chl fluorescence was slightly increased (about 5% compared to control) with the addition of 100 μM NADPH. In contrast, fluorescence decreased by about 35% in the presence of 100 μM $NADP^+$ compared to control. Only the global fluorescence intensity was affected, and no modification of the emission maximum wavelength or of the half-bandwidth of the emission peak was observed. Similar effects of oxidized and reduced NADP were observed in the fluorescence excitation spectra (results not shown). However, the light absorption properties of the thylakoid membranes were not affected. It must be emphasized that the changes in Chl fluorescence induced by $NADP^+$ were fully reversible with addition of NADPH (Figure 2A, insert). This reversibility clearly demonstrates that the changes in Chl fluorescence are not associated with any damage to the thylakoid membranes.

The most relevant subunit where both NADPH and $NADP^+$ are known to interact is FNR located in the PSI complex (*1*, *2*). Heparin and thenoyltrifluoroacetone (TTFA), which are known to specifically bind FNR and inhibit $NADP^+$ reduction (*30*−*33*), also significantly decreased Chl fluorescence (Figure 2A). However, inhibition of PSII electron transport by diuron did not prevent the action of $NADP^+$ on fluorescence in thylakoid membranes as clearly shown in Figure 2B. It should also be noted that oxidized or reduced NADP did not modify the room temperature fluorescence emission spectrum in isolated PSII submembrane fractions (BBY-type) measured in the dark (Figure 3). The above data clearly associate the action of NADP with the PSI complex.

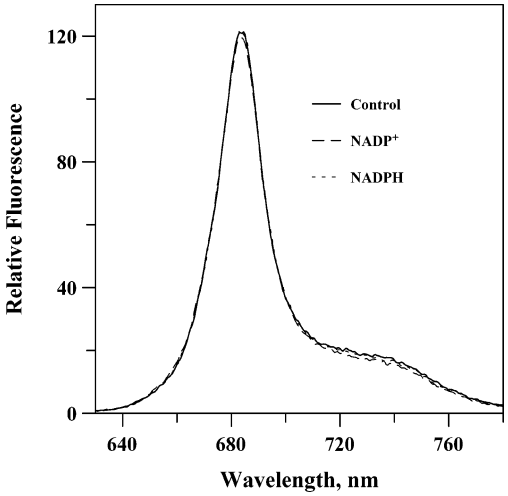

FIGURE 3: Changes in the room temperature (298 K) emission spectra of PSII submembrane fractions with the addition of 100 μM $NADP^+$ or 100 μM NADPH. These experiments were repeated in five different isolations and yielded identical spectra; a typical spectrum is presented.

To study this fluorescence quenching in more detail, we used PSI-enriched submembrane fractions. The PSI submembrane preparation used retains the cytochrome b_6f complex and plastocyanin but is devoid of PSII (*22*). PSI in this preparation should thus operate similarly as in whole thylakoid membranes. It should be noted that the PSI submembrane fractions presented no oxygen evolving activity with PSII electron acceptors such as 2,5-dichlorobenzoquinone and no light-induced variable Chl fluorescence could be detected. The lack of PSII polypeptides in this preparation is clearly shown from the polypeptide profiles of Figure 1 where PSII submembrane fractions are compared with the PSI fractions.

The effects of NADPH and $NADP^+$ observed in PSI preparations confirmed those measured in whole thylakoid membranes. The action of reduced and oxidized NADP at 100 μM was observed when fluorescence was recorded at low temperature (77 K) in the PSI submembrane fractions (Figure 4A). At 77 K, $NADP^+$ decreased fluorescence by 40%. The room temperature (298 K) Chl fluorescence emission spectra presented the characteristic peak at 684 nm and a shoulder around 710 nm (Figure 4B). $NADP^+$ at 100 μM decreased fluorescence by 32% compared to control, and NADPH reversed this quenching. Interestingly, the ratio 684/710 was not modified by the additives; only the global fluorescence intensity was affected. The similar effect of the FNR inhibitor heparin is also shown (Figure 4B). However, oxidized or reduced NAD, an analogue of NADP which is

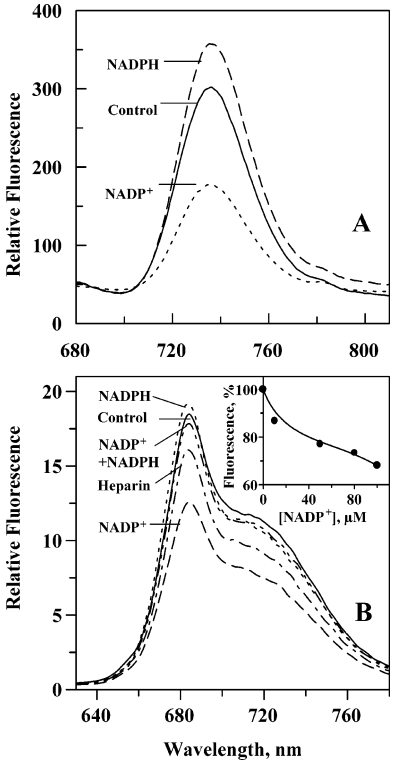

FIGURE 4: (A) Changes in the low temperature (77 K) emission spectra of PSI submembrane fractions with the addition of 100 μM $NADP^+$ or 100 μM NADPH. (B) Room temperature (298 K) emission spectra of PSI submembrane fractions with the addition of 100 μM $NADP^+$, 100 μM NADPH, or 20 μM heparin. Insert: Fluorescence quenching at 684 nm with the addition of various concentrations of $NADP^+$. These experiments were repeated in five different isolations and yielded identical spectra (the variation in intensity was below 5%); a typical spectrum is presented.

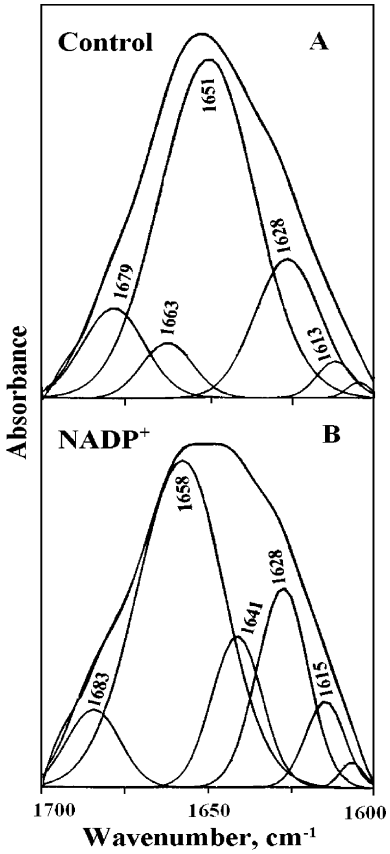

FIGURE 5: Curve-fitted amide I band region (1700−1600 cm^{-1}) and secondary structure determination of the band in PSI submembrane fractions incubated with 100 μM $NADP^+$. Experimental spectra are shown after baseline subtraction together with fitted Gaussian band components.

not a native PSI acceptor, did not produce any significant change of fluorescence intensity. Added spinach ferredoxin (5 μg/mL) had no effect. The fluorescence decrease was studied at various $NADP^+$ concentrations. It is clear from the insert of Figure 4B that relatively low concentrations were required. Above 100 μM $NADP^+$ the quenching further increased but was not fully reversible and probably included some unspecific effects. In principle, compared to whole thylakoid membranes, a greater effect of $NADP^+$ could be expected in PSI preparations where all Chl molecules are associated with PSI. However, we observed similar extents of Chl fluorescence quenching (about 30−35% at 100 μM $NADP^+$; Figures 2A and 4B). The apparently weakened action of $NADP^+$ in PSI submembrane fractions is likely due to the presence of detergent during their isolation that may reduce the accessibility for $NADP^+$ or decrease the amount of membrane-bound FNR molecules.

The modification of fluorescence intensity could be related to a conformational change in the PSI complex. We have studied the conformational changes of the polypeptides in the PSI submembrane fractions using the amide I band of the FTIR spectra measured from control and $NADP^+$-treated preparations. The deconvoluted band profiles are presented in Figure 5. It is clear from Figure 5 that the deconvoluted components are different after addition of $NADP^+$. The assignment of the amide I components is presented in Table 1. The structure of PSI proteins in control samples is compared with samples treated with various additives. The major components in control samples are α-helix (51%) and β-sheet structures (27%). High content in α-helices is expected due to large amounts of intrinsic membrane proteins (*1*, *2*). Random structures are difficult to separate in samples kept in water but were calculated to about 17% in samples kept in D_2O where that proportion was not affected by reduced or oxidized NADP. $NADP^+$ significantly affected the structural components, decreasing α-helices from 51% to 40% and increasing β-sheet structures from 27% to 34%. This effect was reversed after addition of NADPH. Oxidized or reduced NAD was ineffective in producing a conformational change, but heparin caused a conformational change similar to that induced by $NADP^+$ (Table 1).

To study the action of NADP(H) on the photochemical activity of PSI and light-induced oxidation of P700, the reaction center of PSI was analyzed using the absorbance changes at 830 nm. The traces are presented in Figure 6. The action of the various additives was similar to their action on fluorescence. While NADPH alone presented only a negligible effect, $NADP^+$ clearly decreased the extent of absorbance change at 830 nm. The above indicates that the total amount of photooxidizable P700 declined in the presence of $NADP^+$. In control samples (without any addition), the extent and half-time (327 ms) of P700 photooxidation remained identical with different light intensities (from 1.5 to 25 W/m^2). From the maximal extent of absorbance changes shown in Figure 6, it can be calculated that P700 photooxidation in about 25% of the reaction centers is fully but reversibly (with addition of NADPH) impeded.

Table 1: Secondary Structure Determination for PSI Submembrane Fractions Incubated in the Presence of 100 μM $NADP^+$, NADPH, or $NADP^+$ plus NADPH or 20 μM Heparin[a]

amide I component (cm^{-1})	conformation	conformation for PSI (%)	conformation for PSI submembrane fractions incubated with exogeneous additives (%)			
			$NADP^+$	NADPH	$NADP^+$ + NADPH	heparin
1650−1658	α-helix	51 ± 2	40	53	49	43
1613−1640	β-sheet	27 ± 1	34	27	29	31
1641−1648	random	0	17	0	0	9
1663−1678	turn	8 ± 0.2	0	8	9	6
1679−1685	β-antiparallel	14 ± 0.5	9	12	13	11

[a] The results are the averages for three independent experiments. The SD was not more than 5% for all of the components.

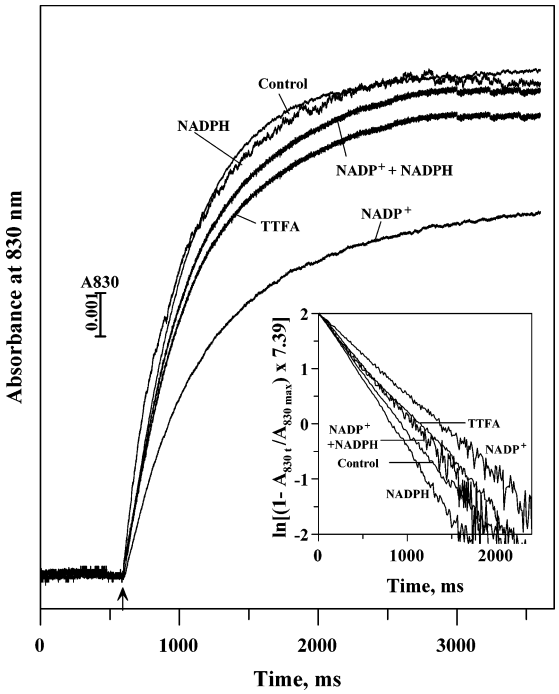

FIGURE 6: Original curves and semilogarithmic plots (insert) of the light-induced rise of absorbance at 830 nm measured in PSI submembrane fractions following the addition of 100 μM $NADP^+$, 100 μM NADPH, or 100 μM TTFA. The sampling rate was 0.3 ms/point. The upward arrow indicates actinic light turned on. The irradiance of white light was 1.5 W m^{-2}. The half-times of ΔA_{830} rise under white light of 1.5 W m^{-2} were 327 ± 7 ms (control), 478 ± 10 ms ($NADP^+$), 297 ± 5 ms (NADPH), 380 ± 6 ms ($NADP^+$ + NADPH), and 393 ± 7 ms (TTFA). The curves represent the average of six measurements; these experiments were repeated in five different isolations and yielded identical curves.

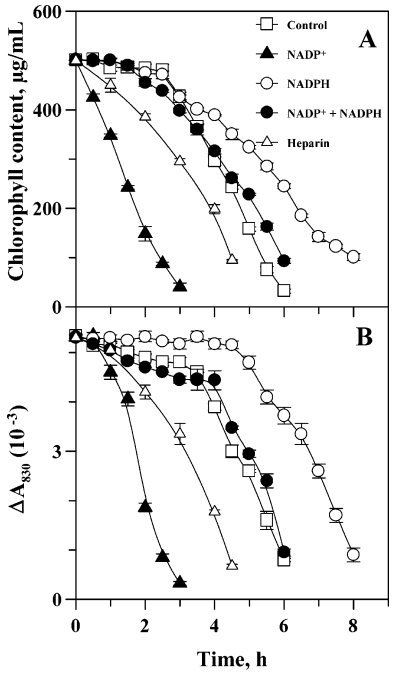

FIGURE 7: Changes in Chl (a + b) content (A) and in the magnitude of light-induced absorbance change at 830 nm (B) during strong light illumination of PSI submembrane fractions with no additive or with the addition of 100 μM $NADP^+$, 100 μM NADPH, 100 μM $NADP^+$ and 100 μM NADPH, or 20 μM heparin. In panel B the values are normalized to the control. Conditions are given in Materials and Methods.

A second action of $NADP^+$ was to increase the half-time for P700 photooxidation (from 327 to 478 ms) in the reaction centers that were able to undergo photooxidation (Figure 6, insert). These two effects of $NADP^+$ were reversed by the addition of NADPH. The inhibitor TTFA (and also heparin) decreased the amount of photooxidizable P700 and increased the half-time for photooxidation (Figure 6).

The involvement of the above changes in photoprotection mechanisms was also investigated. Figure 7 illustrates the changes in total Chl (a + b) content and in the maximum ΔA_{830} magnitude measured during exposure of isolated PSI submembrane fractions to strong white light at 4 °C. The light exposures were performed in the presence of reduced or oxidized NADP. If no additive was present in the suspension, no substantial Chl loss occurred during the first 2 h of light exposure (Figure 7A). Continued light treatment beyond this lag time caused a breakdown of Chl that proceeded linearly. If light exposure was performed in the presence of NADPH, Chl breakdown was somewhat retarded. Unexpectedly, a dramatic acceleration of Chl photobleaching was found in the presence of $NADP^+$. In this case, the lag time completely disappeared. The presence of NADPH together with $NADP^+$ in the suspension of isolated fractions reverted the promoting action of $NADP^+$ on Chl photobleaching. NAD^+ did not influence the pattern of Chl photobleaching, but the inhibitor heparin presented an effect similar to $NADP^+$.

Exposure of isolated PSI submembrane fractions to strong white light at 4 °C also resulted in the loss of ability of P700 to undergo reversible redox changes. Figure 7B demonstrates that the magnitude of the ΔA_{830} signal remained constant during the first 4 h of strong light treatment in the absence of additive. This indicated the unchanged amount of photooxidizable P700 during this lag time period. However, more prolonged irradiation caused a rapid decline in ΔA_{830}. Similar to the results observed for total Chl content, NADPH retarded the onset of fast white light-induced decline in P700 photooxidation, whereas $NADP^+$ or heparin dramatically

accelerated the loss of PSI photochemistry. Added together with $NADP^+$, NADPH nullified the $NADP^+$-induced response. Again, the addition of NAD^+ to the suspension presented no significant effect.

DISCUSSION

To our knowledge, this is the first report that shows significant control over light energy dissipation processes and photochemical activity in PSI by $NADP^+$/NADPH. The quenching induced by $NADP^+$ was clearly associated with PSI but was also occurring in whole thylakoid membranes of pea or spinach, showing the physiological relevance of this process. It should be noted that this effect of $NADP^+$ could not be due to its physiological role as an electron acceptor in PSI because ferredoxin, which is required for electron transfer between PSI and FNR, is a highly soluble polypeptide that is lost during isolation of the submembrane fractions. The similar action observed with inhibitors of $NADP^+$ reduction such as heparin, a non-redox-active compound (*34*), constitutes further evidence in favor of another type of mechanism that does not involve a redox control.

The reversible conversion of about 20% of the α-helices to mainly *β*-sheet-like structures (Table 1) in the polypeptides of PSI indicates a significant conformational change that could account for the decreased fluorescence intensity. It is known from crystal structure analysis that binding of $NADP^+$ to FNR induces a conformational change in the protein (*35*). As isolated stromal fractions of PSI contain this NADP-specific terminal enzyme of the electron transport chain (*36*), we can propose that the binding of $NADP^+$ with FNR initiates macroscopic changes in whole or part of the PSI complex. This binding must act as a trigger to induce the modification of the protein structure. The decreased fluorescence intensity in the presence of heparin and TTFA, which are known to bind with FNR (*31*−*34*), indicates that some effect of these inhibitors on the structure of FNR is similar compared to $NADP^+$. On the other hand, NADPH, likely through its own binding to FNR, removed the action of $NADP^+$.

The partial unfolding of α-helices (Figure 5) that occurs upon binding of $NADP^+$ to FNR should increase intermolecular distances and modify mutual orientations between the various cofactors in the PSI complex. FNR was reported to bind with the PsaE subunit of PSI, the latter being bound to the reaction center heterodimer protein complex of PsaA/PsaB subunits (*37*). Even though the proteins affected by the conformational changes detected by FTIR spectroscopy cannot be identified, it is clear that reaction center polypeptides, which are in closed contact with FNR, should be primarily affected. The increased distances between the primary donor P700 and its electron acceptors and/or between antenna Chls and the reaction center, or a departure from their favorable mutual orientations, could explain the greater half-time for P700 photooxidation. In some centers, the distance between P700 and its primary acceptor or between P700 and the neighboring Chl molecules in charge of transferring excitation energy to the reaction center may become large enough to fully impair P700 photooxidation. This would explain why about 25% of reaction centers could not be photooxidized in the presence of $NADP^+$ (see Figure 6).

The above changes in structure of PSI can also explain the reduced Chl fluorescence. It was shown from reconstituted complexes that LHC-680 (composed of Lhca2 and Lhca3) and Lhca1 of LHC-730 have a fluorescence maximum at 686 nm whereas only Lhca4 fluoresces with a maximum at 725 nm (*38*, *39*). Thus, our data did not present any indication of a disconnection between the peripheral antenna and the core complex that would have resulted in an increased intensity at the fluorescence emission peak of 684 nm in the PSI submembrane fractions. In fact, the general shape of the fluorescence spectra was not modified in the presence of $NADP^+$. Hence, the decreased fluorescence yield likely results from the reduced efficiency of energy transfer between antenna Chl and the reaction center P700, which presented decreased rates of photooxidation, and possibly from a general decrease of energy transfer efficiency among pigment molecules.

Even though $NADP^+$ binding to PSI caused an increased yield of nonradiative dissipation of absorbed energy shown as fluorescence quenching in Figures 2 and 4, this was not effective to provide photoprotection under strong illumination. On the contrary, Chl photobleaching and inhibition of P700 photooxidation observed under strong light were greatly accelerated in the presence of $NADP^+$-induced quenching (Figure 7). Besides P700, red Chl forms and carotenoids present in LHCs and in the core complex of PSI were also associated with protection against excess light (*39*−*41*). It is possible that the conformational changes in the presence of $NADP^+$ decreased the efficiency of energy transfer to P700 and other pigments, thus diminishing their protective role. However, when energy transfer was restored by the addition of NADPH, photodamage was retarded (see Figure 7).

The physiological implications of the above conformational changes leading to the $NADP^+$-induced fluorescence quenching and decreased rates of P700 photooxidation, together with the NADPH-induced reversal of these effects, should be debated in future research. However, the concept that a proper redox poising of the intersystem electron carriers coinciding with moderate reduction of the plastoquinone pool is required for the regulation of ferredoxin-dependent cyclic electron transport is well accepted (*42*). It is also well-known that NADPH promotes cyclic electron transport (*11*). Thus, it is tempting to associate an increased need for P700 turnover in the conditions of high NADPH concentration where both linear and cyclic electron transport reactions have to be supported by PSI to reestablish the appropriate chloroplastic ATP/NADPH ratio. In contrast, at elevated $NADP^+$ concentration only linear electron transport should be supported. In these conditions, a decreased energy flow to P700 or even its reversible disconnection from the electron transport chain due to the NADP-induced conformational changes may increase the reduction state of the plastoquinone pool above that acceptable for active cyclic electron transport. That could also provide photoprotection to the reaction center under specific conditions.

ACKNOWLEDGMENT

The authors thank Drs. N. Murata and G. Samson for useful discussion of this work, Dr. S. Hotchandani for critical reading of the paper, and J. Harnois for helpful professional assistance.

REFERENCES

1. Nechustai, R., Eden, A., Cohen, Y., and Klein, J. (1996) in *Oxygenic Photosynthesis*: *The Light Reactions* (Ort, D. R., and Yocum, C. F., Eds.) pp 289−311, Kluwer Academic Publishers, Dordrecht, The Netherlands.
2. Jordan, P., Witt, H. T., Klukas, O., Saenger, W., and Krauss, N. (2001) *Nature 411*, 909−917.
3. Saenger, W., Jordan, P., and Krauss, N. (2002) *Curr. Opin. Struct. Biol. 12*, 244−254.
4. Scheller, H. V., Naver, H., and Moller, B. L. (1997) *Physiol. Plant. 100*, 842−851.
5. Croce, R., and Bassi, R. (1998) in *Photosynthesis*: *Mechanisms and Effects* (Garab, G., Ed.) pp 412−424, Kluwer Academic Publishers, Dordrecht, The Netherlands.
6. Buchanan, B. B. (1980) *Annu. Rev. Plant Physiol. 31*, 341−374.
7. Satoh, K., and Katoh, S. (1980) *Plant Cell Physiol. 21*, 907−916.
8. Leegood, R. C., Walker, D. A., and Foyer, C. H. (1985) in *Photosynthetic Mechanisms and Environment* (Barber, J., and Baker, N. R., Eds.) pp 189−258, Elsevier Publishers, Amsterdam, The Netherlands.
9. Bukhov, N. G., and Carpentier, R. (1996) *Photosynth. Res. 47*, 13−20.
10. Bendall, D. S., and Manass, R. S. (1995) *Biochim. Biophys. Acta 1229*, 23−38.
11. Joët, T., Cournac, L., Peltier, G., and Havaux, M. (2002) *Plant Physiol. 128*, 760−769.
12. Horton, P., Ruban, A. V., and Walters, R. G. (1996) *Annu. Rev. Plant Physiol. Mol. Biol. 47*, 655−684.
13. Haldrup, A., Jensen, P. E., Lunde, C., and Sheller, H. V. (2001) *Trends Plant Sci. 6*, 301−305.
14. Gilmore, A. M. (1997) *Physiol. Plant. 99*, 127−209.
15. Carpentier, R. (1997) in *Handbook of Photosynthesis* (Pessarakli, M., Ed.) pp 443−450, Dekker Publishers, New York.
16. Aro, E. M., Virgin, I., and Andersson, B. (1993) *Biochim. Biophys. Acta 1143*, 113−134.
17. Powles, S. B. (1984) *Annu. Rev. Plant Physiol. 35*, 15−44.
18. Ohad, I., Sonoike, K., and Andersson, B. (2000) in *Probing Photosynthesis: Mechanisms, Regulation and Adaptation* (Yunus, M., Pathre, U., and Mohanty, P., Eds.) pp 293−309, Taylor & Francis, London, England.
19. Goetze, D. C., and Carpentier, R. (1990) *Photochem. Photobiol. 52*, 1057−1060.
20. Berthold, D. A., Babcock, G. T., and Yocum, C. F. (1981) *FEBS Lett. 134*, 231−234.
21. Rashid, A., Bernier, M., Pazdernick, L., and Carpentier, R. (1991) *Photosynth. Res. 30*, 123−130.
22. Peters, F. A. L. J., Van Spanning, R., and Kraayenhof, R. (1983) *Biochim. Biophys. Acta 724*, 159−165.
23. Boucher, N., Harnois, J., and Carpentier, R. (1990) *Biochem. Cell Biol. 68*, 999−1004.
24. Porra, R. J., Thompson, W. A., and Kriedemann, P. E. (1989) *Biochim. Biophys. Acta 975*, 384−394.
25. Hui, Y., Jie, W., and Carpentier, R. (2000) *Photochem. Photobiol. 72*, 508−512.
26. Rajagopal, S., Bukhov, N. G., and Carpentier, R. (2002) *J. Photochem. Photobiol. 74*, 295−302.
27. Vandenbussche, G., Celercs, A., Curstedt, T., Johansson, J., Jorvall, H., and Ruysshaert, J. M. (1992) *Eur. J. Biochem. 203*, 201−209.
28. Ahmed, A., Tajmir-Riahi, H. A., and Carpentier, R. (1995) *FEBS Lett. 363*, 65−68.
29. Bukhov, N. G., Egorova, E., and Carpentier, R. (2002) *Planta 215*, 812−820.
30. Shahak, Y., Crowther, D., and Hind, G. (1981) *Biochim. Biophys. Acta 636*, 234−243.
31. Cleland, R. E., and Bendall, D. S. (1992) *Photosynth. Res. 34*, 409−418.
32. Teicher, H. B., and Scheller, H. V. (1998) *Plant Physiol. 117*, 525−532.
33. Hosler, J. P., and Yocum, C. F. (1985) *Arch. Biochem. Biophys. 236*, 473−478.
34. Andersen, B., Scheller, H. V., and Moller, B. L. (1992) *FEBS Lett. 311*, 169−174.
35. Hermoso, J. A., Mayoral, T., Faro, M., Gomez-Moreno, G., Sanz-Aparicio, J., and Medina, M. (2002) *J. Mol. Biol. 319*, 1133−1142.
36. Andersen, B., Scheller, H. V., and Moller, B. L. (1992) *FEBS Lett. 311*, 169−173.
37. Schmid, V. H. R., Cammarata, K. V., Bruns, B. U., and Schmidt, G. W. (1997) *Proc. Natl. Acad. Sci. U.S.A. 94*, 7667−7672.
38. Melkozernov, A. N., Schmid, V. H. R., Schmidt, G. W., and Blankenship, R. E. (1998) *J. Phys. Chem. B 102*, 8183−8189.
39. Siefermann-Harms, D. (1987) *Physiol. Plant. 69*, 561−568.
40. Stahl, U., Tusov, V. B., Paschenko, V. Z., and Voigt, J. (1989) *Biochim. Biophys. Acta 973*, 198−204.
41. Jennings, R. C., Garlaschi F. M., Finzy, L., and Zucchelli, G. (1996) *Photosynth. Res. 47*, 167−173.
42. Arnon, D. I., and Chain, P. K. (1977) *Proc. Natl. Acad. Sci. U.S.A. 102*, 133−138.

BI034949K